Geomorphology 407 (2022) 108228

Contents lists available at ScienceDirect

Geomorphology

journal homepage: www.journals.elsevier.com/geomorphology

Late Cenozoic channel migration of the proto-Yangtze River in the delta region: Insights from cosmogenic nuclide burial dating of onshore boreholes

Yu Liu [a,b], Xianbin Liu [c], Shijie Wang [a,b], Sheng Xu [d], Rob M. Ellam [d,e], Derek Fabel [e], Jing Chen [f,*]

[a] State Key Laboratory of Environmental Geochemistry, Institute of Geochemistry, Chinese Academy of Sciences, Guiyang 550081, China
[b] Puding Karst Ecosystem Research Station, Chinese Academy of Sciences, Puding 562100, China
[c] School of Resource and Environmental Engineering, Ludong University, Yantai 264025, China
[d] Institute of Surface-Earth System Science, School of Earth System Science, Tianjin University, Tianjin 300072, China
[e] Scottish Universities Environmental Research Centre, East Kilbride G75 0QF, United Kingdom
[f] State Key Laboratory of Estuarine and Coastal Research, East China Normal University, Shanghai 200062, China

ARTICLE INFO

Keywords:
$^{26}Al/^{10}Be$ burial age
Channel migration
Yangtze River Delta
Late Cenozoic
Sediment provenance change

ABSTRACT

A thorough magnetostratigraphic chronology of the Yangtze River Delta is problematic due to coarse-grained (i.e., poorly magnetized) deposits and sedimentary discontinuity. This study presents cosmogenic nuclide data which facilitate $^{26}Al/^{10}Be$ burial dating to determine the absolute age of horizons from four previously reported long onshore boreholes in the Yangtze Delta region that record sediment provenance change to the Yangtze River. Dates obtained close to the provenance change horizons in boreholes RGK15 and ZKJ39 from the northern delta were 4.99 (+1.26/−0.81) Ma and 4.74 (+0.94/−0.70) Ma, the oldest radiometric ages of borehole sediments yet to date. The provenance change horizon in boreholes LQ19 and LQ11 in the southern delta were dated to 0.94 (+0.17/−0.16) Ma and 0.57 ± 0.17 Ma, respectively. These new ages combined with previous lithofacies and provenance studies imply that the proto-Yangtze River first entered the northern delta prior to ~5 Ma, then migrated gradually southward to the present estuary location after 0.94 Ma and moved even further south at 0.57 Ma. The southward migration history of the proto-Yangtze River channel sheds lights not only on the tectonic subsidence widely occurring on the east China coast during the Quaternary, but also on the somewhat controversial connection history of the Yangtze River to the East China Sea.

1. Introduction

As a result of India-Eurasia collision starting in the early Cenozoic, uplift of the Tibetan Plateau has not only changed crustal deformation and atmospheric circulation patterns (e.g., Molnar and Tapponnier, 1975; Molnar et al., 1993; Chung et al., 1998; An et al., 2001; Tapponnier et al., 2001; Wang et al., 2008) but also changed the regional topographical gradient, with eastern Asia reversing its regional tilt from westward to eastward (Wang, 2004). Reversal of the continental gradient likely triggered reorganization of major river systems (Brookfield, 1998; Clark et al., 2004). Originating on the eastern Tibetan Plateau and flowing into the East China Sea, the Yangtze River is one of the world's longest rivers. The dramatic changes of the macroscopic geomorphology of China imposed in the Cenozoic are recorded in the evolution of the Yangtze River; while these have been extensively studied for more than a century, their implications remain controversial.

The Yangtze River deltaic sedimentary record is a significant repository of drainage information, providing potential insights into Yangtze River evolution. Based on "source to sink" theory, various provenance approaches have been applied to the delta sedimentary sequence. Previous studies traced the provenance of the Yangtze River through the late Cenozoic, using sediment provenance proxies such as heavy minerals, clay minerals, geochemistry, magnetism and zircon geochronology (Fan et al., 2005; Yang et al., 2006; Chen et al., 2009; Gu et al., 2014; Zheng et al., 2013; Liu et al., 2018; Yue et al., 2019; Yu et al., 2020). A consensus conclusion based on paleomagnetic

* Corresponding author.
E-mail address: jchen@geo.ecnu.edu.cn (J. Chen).

https://doi.org/10.1016/j.geomorph.2022.108228
Received 11 October 2021; Received in revised form 25 March 2022; Accepted 26 March 2022
Available online 1 April 2022

chronology (Liu et al., 2018; Yue et al., 2019; Yu et al., 2020) is that a major provenance shift related to the Yangtze River occurred during the Pliocene to Early Pleistocene, but happened earlier in the north delta than in the south delta.

Paleomagnetic dating provides relative chronology by comparison of polarity reversals recorded in local cores with the well-established global standard sequence. A successful paleomagnetic chronology depends on the continuity of the stratigraphic sequence in the local cores. However, coarse fluvial deposits frequently occur in the Plio-Pleistocene stratigraphy of the Yangtze River Delta, implying erosive activity and consequent stratigraphic discontinuity which will deleteriously affect sampling continuity and hence paleomagnetic data integrity (see inclination and polarity in Fig. 2). Thus, some important boundary or polarity events used to assemble a chronological model for the major provenance shift are ambiguous and potentially unreliable. Key stratigraphic markers related to the timing of the shift in the northern and southern deltas that are less than definitive include the Gauss-Matuyama reversal and the Jaramillo subchron (Chen et al., 2009; Gu et al., 2014; Liu et al., 2018; Yue et al., 2019; Yu et al., 2020). This is a common problem with the late Cenozoic chronology of the delta region, and limits our understanding of the geomorphological evolution of the Yangtze River and its delta (Fan et al., 2005; Yang et al., 2006; Chen et al., 2009; Gu et al., 2014; Liu et al., 2018; Yue et al., 2019; Yu et al., 2020).

Coarse deposits are nonideal for magnetostratigraphy but are the preferable medium for in-situ terrestrial cosmogenic nuclide (TCN) radiometric dating. TCN-dating has become increasingly reliable as a method for dating geomorphic surfaces and measuring process rates over 10^2–10^6 year time scales (Balco et al., 2008; Liu et al., 2013; Granger, 2014; McPhillips et al., 2016; Blard et al., 2019). In view of the importance of the site and its stratigraphy, an attempt to date provenance shift layers from four onshore boreholes in the Yangtze River Delta was performed by cosmogenic ^{26}Al—^{10}Be burial dating. We aim to provide an independent check on the results of previous magnetostratigraphy. In particular, we try to assess the radiometric ages of these provenance shift sediments to provide insights into the Yangtze River channel migration history in the estuarine region and implications for the evolution of the Yangtze River drainage basin.

2. Geological setting

The Yangtze River, with a length of ~6300 km, drains eastward through three major topographic steps within China and discharges into the East China Sea (Fig. 1a). The Yangtze River basin covers a vast area (~1.8 × 10^6 km^2), with substantial topographical contrast reflecting complex geology (Fig. 1a). The Yangtze water course may be divided into (upper) the section from the headwaters to the east end of the Three Gorges (Yichang city), (middle) from Yichang city to Hukou city (estuary of the Lake Poyang) and (lower) from Hukou city to the East China Sea. The middle and lower Yangtze River sections are approximately 1200 km in length, and along the full length of the river the mean altitude of drainage decreases from 2000 m to under 500 m. Changing topography is reflected by flow velocity which is quickly reduced to develop a meandering river. Three large basins are mainly distributed in the three reaches, the upstream Sichuan Basin (SCB) in the west is connected to the middle Jianghan Basin (JHB) by the Three Gorges, which is in turn connected to the lower Subei-South Yellow Sea Basin (SSYSB) to the north of the modern Yangtze River Delta. Apart from a few hundred meters of Quaternary sediments deposited in the western Chengdu Plain, the SCB was characterized by widespread erosion during the Cenozoic (Richardson et al., 2008). In contrast, thick fluvial and lacustrine sediments were deposited in the downstream JHB (Wang et al., 2014) and SSYSB basins (Qiang et al., 1997).

Geologically, the Yangtze River drainage basin comprises several tectonic systems. From west to east, these include the Qamdo Block, the Songpan-Garze terrane, the Qinling-Dabie orogenic belts, the Yangtze Craton and the Cathaysia Block (Fig. 1a). The upper reaches are dominated by Paleozoic-Mesozoic carbonate and clastic rocks, with a large-scale Mesozoic basaltic outcrop (the Emeishan Basalt; Fig. 1a) and some Cenozoic felsic igneous rocks (Changjiang Water Resources Commission, 1999). Previously, the Emeishan Basalt, which has characteristic geochemistry and magnetic properties (high χlf, SIRM and S-ratio, and low χARM/χlf and χARM/SIRM), has been widely used as a key tracer of the upper reach provenance in downstream basins, and is indicative of the connection of the Three Gorges (e.g., Zhang et al., 2008; Chen et al., 2009; Gu et al., 2014; Shao et al., 2015; Liu et al., 2018). The middle and lower reaches are primarily dominated by Paleozoic-Mesozoic sedimentary rocks and unconsolidated Quaternary sediments, with some felsic igneous rocks and metamorphic rocks (Changjiang Water Resources Commission, 1999).

The Yangtze River Delta (30°20′-32°30′ N , 119°24′-122°30′ E) lies east of the Yangtze Block where the channel is no longer controlled by bedrock and is the most downstream terrestrial depocenter before the Yangtze River flows into the sea. The Yangtze River Delta depression was formed due to the extension caused by Pacific-Eurasia convergence during the Paleocene (Ren et al., 2002). The modern delta plain was

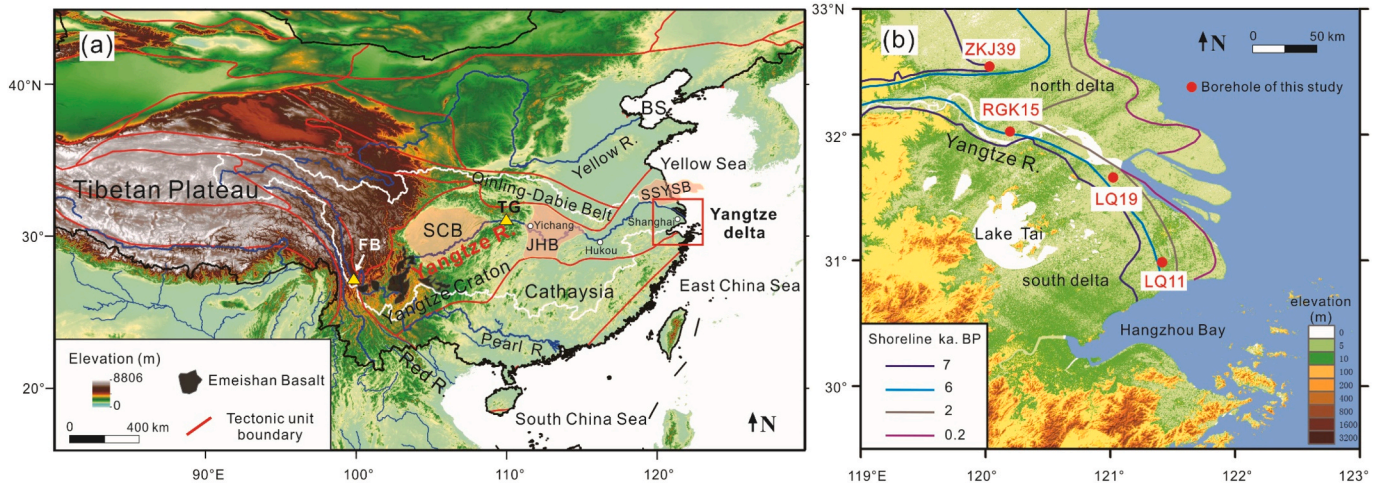

Fig. 1. (a) Geomorphologic map of East Asia showing the Yangtze River drainage basin (white line shows the basin boundary) and location of the Yangtze River Delta in the red box. BS: Bohai Sea; SSYSB: Subei-South Yellow Sea Basin; SCB: Sichuan Basin; JHB: Jianghan Basin; FB: First Bend; TG: Three Gorges. (b) Schematic map of four studied borehole locations (red dots) in the modern Yangtze River Delta. The position and age of the old shorelines are after Saito et al. (2001).

formed by 1.7×10^{12} tons of sediments transported by the Yangtze River over the past 7 ka as sea level evolved towards its present position (Fig. 1b; Saito et al., 2001). The Yangtze River Delta can usefully be subdivided into northern and southern delta plains separated by the main channel (Fig. 1b). The delta plain terrain is low and flat with an average altitude of approximately 4 m. Except for a few bedrock monadnocks in the southern plain, most of the area is covered by poorly-consolidated late Cenozoic sediments that deposited unconformably on bedrock with a thickness of >1000 m in the north and 200–400 m in the south delta (Chen and Stanley, 1995).

3. Material and methods

3.1. Borehole description and sampling

Core ZKJ39 (32°30′11″N, 120°02′05″E) penetrated 322.2 m into the north Yangtze River Delta (Fig. 1b) and did not reach bedrock. Its lithologies, sedimentary facies, heavy minerals, zircon morphological characteristics, magnetostratigraphy, magnetic properties and foraminiferal assemblages are described in Yue et al. (2016) and Liu (2018) (Fig. 2). These previous studies indicate that a significant provenance shift occurred at a depth of 235 m with the upper sediments derived from the Yangtze River. A sand subsample at a depth of 231.5 m was collected from this core for ^{26}Al—^{10}Be burial dating.

Core RGK15 (32°7′1″N, 120°28′59″E) was recovered by rotary drilling from the vertex of the north Yangtze River Delta plain (Fig. 1b). The core reached 318 m depth and reached Cretaceous bedrock. Detailed lithologies, sedimentary facies and chronology determined by paleomagnetic, optically stimulated luminescence (OSL) and AMS ^{14}C methods were described in Yu et al. (2020) (Fig. 2). Heavy minerals and zircon U—Pb ages reveal a significant provenance shift at a depth of 272 m, which is ~2.6 Ma according to the paleomagnetic chronology (Yu et al., 2020). A sand layer at a depth of 269 m, was collected for ^{26}Al—^{10}Be burial dating.

Core LQ19 (31°28′22″N, 121°19′44″E) was drilled in northwest Shanghai city, to the west of the present Yangtze River channel (Fig. 1b). The core was continuously drilled to a depth of 330.9 m and reached Cretaceous bedrock. Lithologies, sedimentary facies, magnetostratigraphy, magnetic properties and foraminiferal assemblages are described in Liu (2018) (Fig. 2). Many magnetic parameters show an abrupt change at a depth of 225 m suggesting that the sediment beneath this depth was of local provenance and sediment above 225 m was dominated by the Yangtze River deposition (Liu, 2018). Two sand samples from depths of 225 m and 223 m were collected for ^{26}Al—^{10}Be burial dating.

Core LQ11 (31°01′43″N, 121°22′7″E) with a continuous 301 m length down to Jurassic bedrock was recovered by rotary drilling from the southern Yangtze River Delta plain in Shanghai city (Fig. 1b). Sedimentary facies, lithology, magnetic properties, magnetostratigraphy, organic carbon analysis and foraminifera identification were recorded for this core, and are described in detail by Liu et al. (2018). Magnetic properties characterized by high χ_{lf}, SIRM, S_{-300} and low χ_{ARM}/SIRM suggest a profound sediment provenance change at a depth of 145 m with an inferred palaeomagnetic age of 1.0–1.2 Ma (Liu et al., 2018). A sand layer at a depth of 145 m was subsampled for ^{26}Al—^{10}Be burial dating.

3.2. Sample preparation and analysis

The five coarse sand samples from four boreholes were sieved to 0.25–0.5 mm. Quartz was separated and purified in the State Key Laboratory of Environmental Geochemistry (SKLEG), Institute of Geochemistry, Chinese Academy of Sciences. Beryllium and aluminum extraction and purification, accelerator mass spectrometry (AMS) measurement of ^{26}Al and ^{10}Be concentrations, and total Al determination by inductively coupled plasma optical emission spectrometry (Thermo Fisher Scientific iCAP 7400, assigned 3% uncertainty) were all performed at the Scottish Universities Environmental Research Centre (SUERC). The 0.125–0.25 mm size fraction was used for quartz purification by selective chemical dissolution (Kohl and Nishiizumi, 1992). The purified quartz (10–20 g) was dissolved in a solution of concentrated HF. Approximately 0.2 mg Be carrier was added to the samples and a procedural blank. Al carrier (1.0 mg) was added only to the blank. Al and Be were extracted and separated by ion chromatography and

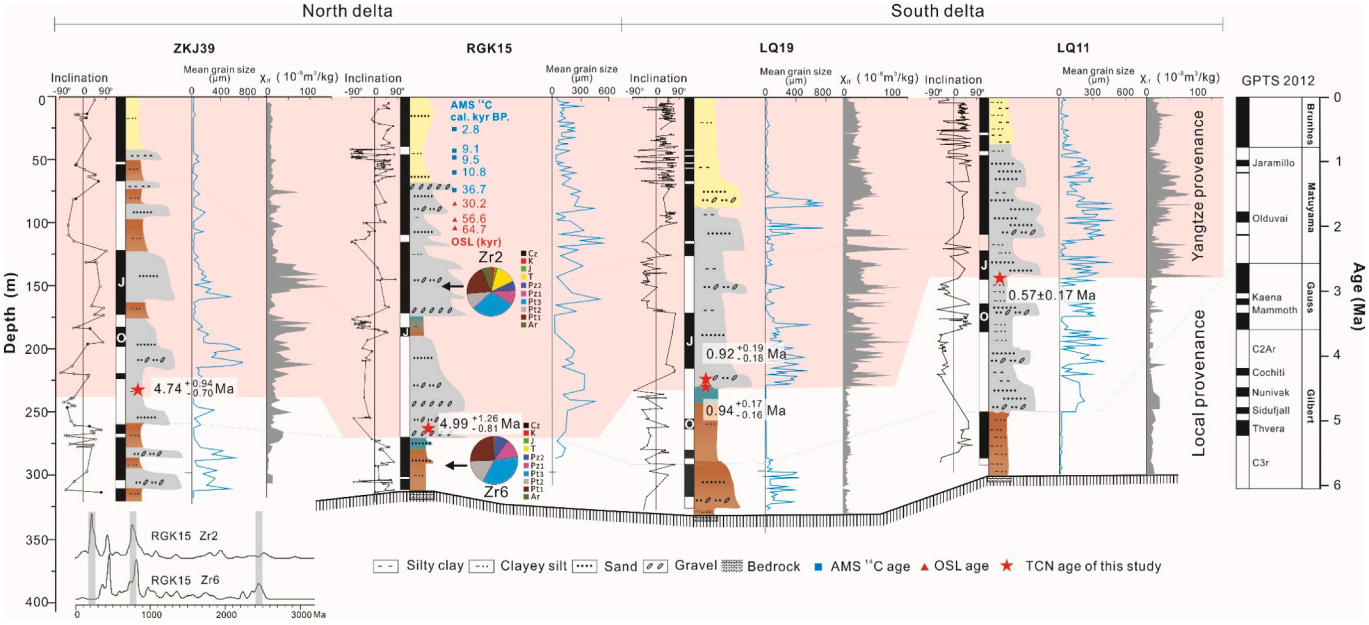

Fig. 2. Lithology, magnetostratigraphy, mean grain size, magnetic susceptibility (χ_{lf}) and absolute age of the studied boreholes in the modern Yangtze River Delta. The geomagnetic polarity timescale (GPTS) is from Hilgen et al. (2012) and Pillans and Gibbard (2012). Pink shading marks higher magnetic susceptibility in the upper cores and indicates Yangtze River-derived provenance. Normalized relative age probability diagrams of detrital zircons from depths of 150 m (Zr2) and 290 m (Zr6) in core RGK15 and their proportions are shown in pie charts. Data of the detrital zircon, ^{14}C age and OSL age of core RGK15 are all sourced from Yu et al. (2020).

selectively precipitated as hydroxides. The precipitates were oxidized at 800 °C. Al_2O_3 and BeO were mixed with Ag and Nb matrices respectively with weight ratios of Al_2O_3: Ag = 1: 2 and BeO: Nb = 1: 6 for AMS analysis (Xu et al., 2015). The procedural blank processed in association with the samples has a $^{10}Be/^{9}Be$ of $(5.63 \pm 0.66) \times 10^{-15}$ and $^{26}Al/^{27}Al$ of $(1.12 \pm 0.79) \times 10^{-15}$. The measured $^{26}Al/^{27}Al$ and $^{10}Be/^{9}Be$ ratios are normalized to primary standards Z92-0222 with a nominal $^{26}Al/^{27}Al$ ratio of 4.11×10^{-11} and NIST SRM 4325 with a nominal $^{10}Be/^{9}Be$ ratio of 2.79×10^{-11}, respectively.

3.3. $^{26}Al/^{10}Be$ simple burial dating

Cosmogenic nuclide burial dating uses measurements of the concentration of cosmic rays produced terrestrial ^{10}Be and ^{26}Al in samples that were exposed at Earth's surface prior to deposition and subsequent shielding from cosmic rays. Once buried, the ^{26}Al and ^{10}Be concentrations decrease due to radioactive decay, and the faster decay of ^{26}Al results in a decrease in $^{26}Al/^{10}Be$. The $^{26}Al/^{10}Be$ ratio is used to derive a burial age assuming closed system behavior (Granger and Muzikar, 2001; Granger, 2006; Granger, 2014).

The long-term concentration (N_i) of ^{26}Al or ^{10}Be in quartz that is exposed near the surface and then buried follows the relationship:

$$N_i = N_{i,inh} e^{(-t/\tau_i)} + N_{i,pb} \quad (1)$$

where subscript i represents either ^{26}Al or ^{10}Be, *inh* indicates inheritance prior to burial, t is burial age, τ is the radioactive mean life and *pb* indicates the total post-burial production. In a landscape that is eroding steadily at a rate E, the inherited nuclide concentration is:

$$N_{i,inh} = P_n / (1/\tau_i + \rho E/\Lambda_n) + P_\mu / (1/\tau_i + \rho E/\Lambda_\mu) \quad (2)$$

where P_n, P_μ and Λ_n, Λ_μ are the production rates (atoms/g/yr) and penetration lengths (g/cm^2) due to neutrons and muons (negative muon and fast muon), respectively. ρ indicates rock density. Simple burial dating assumes that the sample was exposed at the surface with a high concentration of inherited nuclides and was then buried deeply enough (typically more than 10 m) that post-burial production can safely be ignored. In this case, Eq. (1) simplifies to

$$N_{26}/N_{10} = (N_{26,inh}/N_{10,inh}) e^{-t(1/\tau_{26} - 1/\tau_{10})} \quad (3)$$

Eq. (2) and Eq. (3) can be solved iteratively for converging the solution of burial age t and pre-burial erosion rate E.

The basic premise of burial dating is that sediment is buried deeply enough to avoid significant post-burial nuclide production and has a simple exposure history prior to burial. Thus, simple burial dating is ideal for dating cave sediments or very thick fluvial deposits. However, complex exposure-burial histories cannot be ruled out, making all burial ages maximum ages. The current burial dating method limits range roughly between 0.1 and 5 Ma (Granger, 2014).

Our sampled boreholes are located at the river-mouth of the Yangtze River, its upstream area is large and the landscape is complicated (Fig. 1a). Therefore, the average latitude (30°N) and average altitude of the drainage basin (2000 m) were taken as the best approximation to calculate production rates. Cosmogenic nuclide production rates were assumed to be constant for the basin and were calculated as $P_{10} = 15.0$ atoms/g/yr and $P_{26} = 101.7$ atoms/g/yr including neutron and muon contributions. Cosmogenic nuclide production rates and burial ages were calculated using the CRONUS-earth online calculator v. 2.3 MATLAB code (Balco et al., 2008). For an assumed rock and overlying sediment density of 2.60 g/cm^3, the exponential penetration length for any nucleon is 160 g/cm^2 (Masarik and Reedy, 1995), whereas negative muon and fast muon penetration lengths are 1510 g/cm^2 and 4320 g/cm^2, respectively (Heisinger et al., 2002a, 2002b). The radioactive mean lives of ^{26}Al ($\tau_{26} = 1.021 \pm 0.024$ Ma; Nishiizumi, 2004) and ^{10}Be ($\tau_{10} = 2.005 \pm 0.017$ Ma; Chmeleff et al., 2010) were used. The burial age calculation assumes a rapid deposition rate and no cosmogenic nuclides post-production.

4. Results and discussion

All analytical results are listed in Table 1 and shown in Fig. 3. The stated errors are 1σ calculated from AMS and ICP-OES uncertainties. Samples RGK15 and ZKJ39 in the northern delta have very low measured $^{26}Al/^{27}Al$ ratios of $0.29 \pm 0.11 \times 10^{-14}$ and $0.40 \pm 0.12 \times 10^{-14}$, respectively. The procedural blank represents 38% and 28% of the ^{26}Al atoms, respectively. Compared with Al, the $^{10}Be/^{9}Be$ ratios of these two samples are four times higher than that of the blank. Low concentrations of both ^{26}Al and ^{10}Be in samples RGK15 and ZKJ39 result in low $^{26}Al/^{10}Be$ ratios with large uncertainties. This effect is most extreme for sample RGK15 with approximately 50% uncertainty and results in the oldest burial age of 4.99 (+1.26/−0.81) Ma. Improved data precision could be achieved by using larger amounts of quartz to increase AMS counting statistics. However, the amount of borehole samples is limited and only a small yield of coarse sand remained after sieving and purification. A similar situation also occurred in the southern delta borehole (LQ19) for which each sample gave only ~10 g of pure quartz. Therefore, 4.99 (+1.26/−0.81) Ma and 4.74 (+0.94/−0.70) Ma with relatively large uncertainties were the best results obtainable from boreholes RGK15 and ZKJ39 respectively. For the southern delta cores, LQ11 has a burial age of 0.57 ± 0.17 Ma while the burial age of core LQ19 at depth of 223 m is 0.92 (+0.19/−0.18) Ma, which is in good agreement with the burial age of 0.94 (+0.17/−0.16) Ma of sediment at a depth of 225 m.

4.1. Comparison of cosmogenic nuclide burial age and magnetostratigraphy of the studied boreholes in the Yangtze River Delta

The magnetostratigraphy of the four studied cores in the Yangtze River Delta (Fig. 2) are derived from Liu et al. (2018), Yu et al. (2020), and Liu (2018). Paleomagnetic analysis of core LQ11 reveals the Gauss normal chron at a depth between 300 m and 252 m, and the Matuyama reversed chron between 252 and 112 m. The Olduvai and Jaramillo subchrons are recognized at depths of 186–160 m and 145–121 m, respectively. The Brunhes normal chron is evident above 112 m. Therefore, the paleomagnetic age of the significant provenance shift to Yangtze River-derived sediments at a depth of 145 m is near the base of the Jaramillo subchron at ~1.0–1.2 Ma (Liu et al., 2018). This age is much older than the $^{26}Al/^{10}Be$ burial age of 0.57 ± 0.17 Ma from the same horizon of core LQ11.

Similarly, three chrons including Gauss, Matuyama and Brunhes were also recognized in other borehole sediments of LQ19, ZKJ 39 and RGK 15 (Fig. 2). For core LQ19, the Olduvai and Jaramillo subchrons are inferred at depths of 260–254 m and 155–148 m, respectively. This means that the provenance shift sediment at a depth of 225 m should be between 1.05 and 1.78 Ma, most likely around 1.0–1.2 Ma (Liu et al., 2018). This is the only paleomagnetic age that is coincident with the cosmogenic burial age of 0.94 (+0.17/−0.16) Ma within uncertainty. The $^{26}Al/^{10}Be$ burial age of the 223 m depth (i.e., 2 m shallower) sand yields a similar age of 0.92 (+0.19/−0.18) Ma, suggesting rapid fluvial deposition.

For core ZKJ39, the correlation of the magnetic polarity sequence to the geomagnetic polarity timescale suggested that the Olduvai and Jaramillo subchrons are inferred at depths of 199–168 m and 151–122 m, respectively (Fig. 2; Liu et al., 2018). Hence, the paleomagnetic age of the provenance shift sediment at a depth of 234.5 m should be older than the Olduvai subchron and younger than the Gauss chron (1.9–2.6 Ma). Our dated sand at a depth of 231.5 m (i.e., 3 m shallower) yields a burial age of 4.74 (+0.94/−0.70) Ma, indicating that the provenance shift event in core ZKJ39 should have occurred earlier than this age. For core RGK15, the Pliocene/Pleistocene boundary occurs at 272 m and the Early/Middle Pleistocene boundary is located at 173 m (~0.78 Ma;

Table 1
Cosmogenic ^{26}Al and ^{10}Be results of the studied boreholes from the Yangtze River Delta.

Borehole	Sample depth (m)	Quartz mass (g)	^{27}Al in quartz (ppm)	^{26}Al/^{27}Al (10^{-14})	^{10}Be/^{9}Be (10^{-14})	Concentration (atoms/g)		^{26}Al/^{10}Be	Model burial age (Ma)
						^{26}Al (10^4)	^{10}Be (10^4)		
LQ11	145	14.98	125 ± 6	15.04 ± 0.82	8.63 ± 0.26	41.81 ± 3.10	8.04 ± 0.28	5.20 ± 0.43	0.57 ± 0.17
LQ19	223	10.04	137 ± 7	10.01 ± 0.59	5.22 ± 0.20	30.41 ± 2.38	6.91 ± 0.32	4.40 ± 0.40	0.92 (+0.19/−0.18)
	225	10.86	114 ± 6	17.10 ± 0.79	7.79 ± 0.27	43.12 ± 2.95	9.91 ± 0.40	4.35 ± 0.35	0.94 (+0.17/−0.16)
RGK15	269	20.98	138 ± 7	0.29 ± 0.11	2.31 ± 0.15	0.76 ± 0.35	1.23 ± 0.12	0.62 ± 0.29	4.99 (+1.26/−0.81)
ZKJ39	231.5	20.17	123 ± 6	0.40 ± 0.12	2.47 ± 0.26	0.98 ± 0.35	1.40 ± 0.20	0.70 ± 0.27	4.74 (+0.94/−0.70)

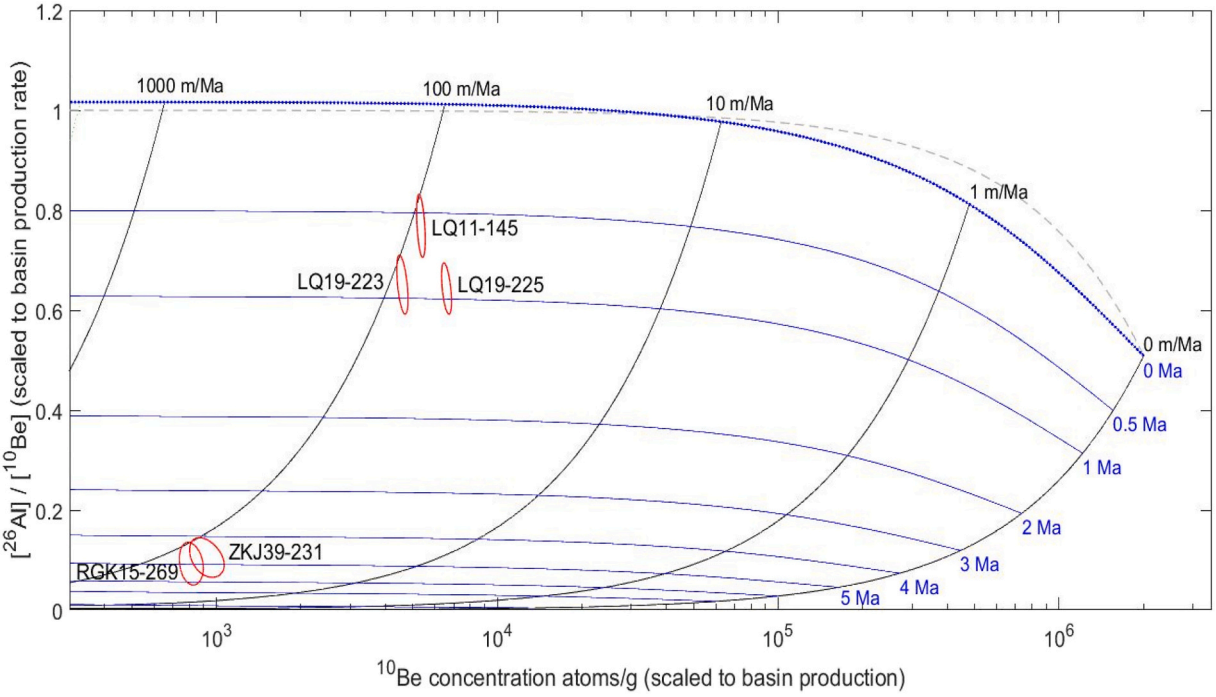

Fig. 3. Cosmogenic nuclide data from the studied boreholes in the Yangtze River Delta, shown on a logarithmic graph of ^{26}Al/^{10}Be versus ^{10}Be concentration.

Fig. 2; Yu et al., 2020). Therefore, the paleomagnetic age of provenance shift sediment at a depth of 272 m should be around 2.60 Ma. However, the cosmogenic ^{26}Al/^{10}Be ratio at a depth of 269 m yields a burial age of 4.99 (+1.26/−0.81) Ma. However, these two apparent old radiometric ages are consistent with most recent detrital zircon geochronology from the East China Sea Shelf Basin, suggesting that the present-day Yangtze River was established in the late Miocene (Fu et al., 2021). Thus, the age constraints from cosmogenic ^{26}Al/^{10}Be offer independent evidence that the paleomagnetic ages of cores ZKJ39 and RGK15 may have been significantly underestimated in previous studies.

Apparently, the magnetostratigraphy of the four studied cores in the Yangtze River Delta are only occasionally in accordance with cosmogenic nuclide absolute ages, and may overestimate or underestimate the sediment deposition age. These discrepancies most likely reflect the complexity of river and ocean sedimentary systems, particularly during the Quaternary. Sediment and mineral compositions vary in estuarine environments, and/or river channel migration results in discontinuous sedimentation and variable deposition rates (Morton, 1984; Chen and Stanley, 1995). Together with coarser fluvial sediments (e.g., sand and pebble) that repeatedly appear in the deposition sequence, especially for the Pliocene and early Pleistocene sediments (Fig. 2), these factors may have significantly affected the reliability of paleomagnetic ages.

4.2. Proto-Yangtze River channel migration in the delta region during the late Cenozoic

The cosmogenic ^{26}Al/^{10}Be burial ages and previous provenance studies of four cores record the channel migration history of the proto-Yangtze River in the delta region during the late Cenozoic (Fig. 4). The modern Yangtze River similar provenance characteristics such as high ferrimagnetic content, diverse heavy mineral assemblages, and multiple peaks of the zircon age spectra, occurred above 235 m and 272 m in cores ZKJ39 and RGK15 of the northern delta and above 225 m and 145 m in cores LQ19 and LQ11 of the southern delta (see Figs. 3 and 5 in Yu et al., 2020; Fig. 2; Wang et al., 2006; Yue et al., 2019). The combination of burial ages of the horizons close to provenance change in these cores suggests that the proto-Yangtze River channel primarily appeared in the northern delta prior to 4.74–4.99 Ma (Figs. 2 and 4a). Later, it migrated southward to the modern river mouth after 0.92–0.94 Ma, and the mainstream channel or possibly just one branch of the channel had moved further southward (where core LQ11 is located) after 0.57 Ma (Fig. 4b). The southward migration of the proto-Yangtze River resulted in abandonment of the original channel in the northern delta, which might have caused sedimentary hiatuses or a rapid decrease in the sediment deposition rate. For core RGK15, the TCN age at a depth of 270 m reaches 4.99 Ma and then decreases to 64.7 ka at a depth of ~110 m based on OSL dating. For core ZKJ39, both the ferrimagnetic content and grain size decreased in the upper part (135–0 m). Today, the south proto-Yangtze River channel (location of core LQ11) has been

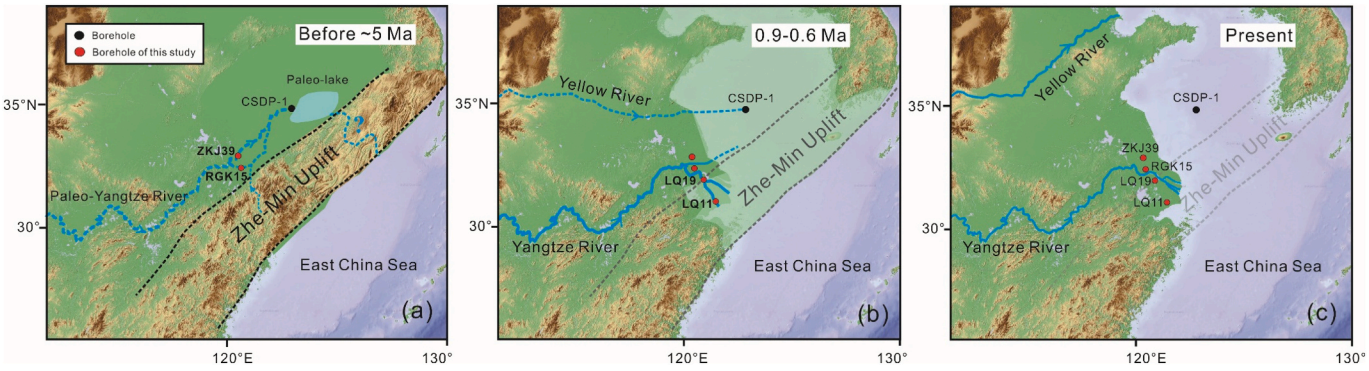

Fig. 4. Time scales of schematic diagrams illustrate the southward migration of the Yangtze River channel in the Yangtze River Delta area. Dashed blue lines represent guessed river channels. (a) Before ~5 Ma, the proto-Yangtze River flowed through the northern delta area (location of cores ZKJ39 and RGK15) into the South Yellow Sea paleolake due to the barrier of the Zhe-Min Uplift. (b) After ~0.9 Ma, the Yangtze River migrated southward and flowed into the East China Sea through the south delta area (location of cores LQ19 and LQ11) due to the Zhe-Min Uplift subsidence. (c) At present, the Zhe-Min Uplift has subsided below sea level and a southern channel of the Yangtze River has disappeared (location of core LQ11).

abandoned with the development of the current channel pattern (Fig. 4c).

This migration history and age interpretation are supported by recent studies on core CSDP-1 in the western offshore area of the South Yellow Sea, which is approximately 300 km northeast of core ZKJ39 (Fig. 4). Magnetostratigraphy together with clay mineral assemblages and Sr—Nd isotopes indicate that sediment in core CSDP-1 was Yangtze River-derived before ~0.8 Ma and then shifted to the Yellow River-derived (Fig. 4b; Liu et al., 2014; Zhang et al., 2019). This conclusion suggests southward migration of the proto-Yangtze River channel after 0.8 Ma, which is generally consistent with the cosmogenic burial ages of this study (~0.9 Ma).

The southward migration of the proto-Yangtze River is likely to have been in response to accelerated tectonic subsidence of the eastern China coast and the Zhejiang-Fujian Uplift (Qin et al., 1989; Chen and Stanley, 1995; Li et al., 2011). The Zhejiang-Fujian Uplift (abbreviated as the Zhe-Min Uplift) extends from Zhejiang and Fujian Provinces of China's southeastern coast to the southern Korean Peninsula, and was associated with the igneous intrusion and eruption activities due to the subduction of the Pacific Plate towards the Eurasian Plate since the Triassic. It was once a high terrain and a natural barrier to the incursion of sea water in eastern China before the Quaternary (Jin and Yu, 1982). Since the early Cenozoic, the Zhe-Min Uplift began to subside gradually under the extended domain of the continental margin. Its accelerated subsidence since the early Pleistocene caused marine transgression in east China, with sea-land interaction first observed in boreholes from the South Yellow Sea no later than 1.7 Ma, and eventual subsidence below sea level at ~0.2 Ma (Wageman et al., 1970; Liu et al., 2014; Yi et al., 2014, 2016; Mei et al., 2016). Therefore, before the early Pliocene (~5 Ma), the Yangtze River Delta region was still elevated, especially in the southern area within the Zhe-Min Uplift, constraining the proto-Yangtze River to flow only through the northern delta region with relatively low altitude and slope. Following Quaternary subsidence of the Zhe-Min Uplift, and particularly accelerated subsidence around 0.8 Ma (Liu et al., 2014, 2016; Mei et al., 2016; Zhang et al., 2019), the proto-Yangtze River channel began to migrate southward arriving at the modern river mouth after ~0.9 Ma.

The new cosmogenic burial ages of this study not only help better understanding the migration history of the Yangtze River channel in the delta area during the Late Cenozoic, but also provide new insights for constraining tectonic subsidence history of eastern China. Further, these results have implications for the broader controversy regarding connection of the Yangtze River to the East China Sea.

5. Conclusion

The important provenance change layer found in four onshore boreholes in the Yangtze River Delta has been dated for the first time using the cosmogenic $^{26}Al/^{10}Be$ burial method. The horizons that sourced sediments from the Yangtze River yield burial ages of 4.99 (+1.26/−0.81) Ma and 4.74 (+0.94/−0.70) Ma in two cores from the northern delta, and 0.94 (+0.17/−0.16) Ma and 0.57 ± 0.17 Ma in another two cores from the southern delta. The new cosmogenic burial ages imply that the proto-Yangtze River channel was first occupied the northern delta area prior to ~5 Ma, and then migrated southward after ~0.9 Ma, which possibly resulted from the tectonic subsidence of the Zhe-Min Uplift during the middle Quaternary.

Declaration of competing interest

The authors declared that they have NO conflicts of interest to this work. We declare that we do not have any commercial or associative interest that represents a conflict of interest in connection with the work submitted.

Acknowledgements

We are grateful to the three reviewers and the editor for their thoughtful and constructive comments and suggestions that greatly improved the manuscript. We thank María Miguens-Rodríguez for cosmogenic nuclide sample preparation. This research was funded by the Strategic Priority Research Program of the Chinese Academy of Sciences (XDB40020300) and the National Natural Science Foundation of China (grant numbers 41473055, 41771226, 41401009 and 41620104004).

References

An, Z.S., Kutzbach, J.E., Prell, W.L., Porter, S.C., 2001. Evolution of Asian monsoons and phased uplift of the Himalaya-Tibetan plateau since late Miocene times. Nature 411, 62–66.

Balco, G., Stone, J.O., Lifton, N.A., Dunai, T.J., 2008. A complete and easily accessible means of calculating surface exposure ages or erosion rates from Be-10 and Al-26 measurements. Quat. Geochronol. 3, 174–195.

Blard, P.H., Lupker, M., Rousseau, M., 2019. Paired-cosmogenic nuclide paleoaltimetry. Earth Planet. Sci. Lett. 515, 271–282.

Brookfield, M.E., 1998. The evolution of the great river systems of southern Asia during the Cenozoic India-Asia collision: rivers draining southwards. Geomorphology 22, 285–312.

Changjiang Water Resources Commission, 1999. Atlas of the Changjiang River Basin. Chinese Atlas Press, Beijing, China (in Chinese).

Chen, Z.Y., Stanley, D.J., 1995. Quaternary subsidence and river channel migration in the Yangtze River Delta plain, eastern China. J. Coast. Res. 11, 927–945.

Chen, J., Wang, Z.H., Chen, Z.Y., Wei, Z.X., Wei, T.Y., Wei, W., 2009. Diagnostic heavy minerals in Plio-Pleistocene sediments of the Yangtze Coast, China with special reference to the Yangtze River connection into the sea. Geomorphology 113, 129–136.
Chmeleff, J., Blanckenburg, F., Kossert, K., Jakob, D., 2010. Determination of the 10Be half-life by multi collector ICP-MS and liquid scintillation counting. Nucl. Inst. Methods Phys. Res. B 268, 192–199.
Chung, S.L., Lo, C.H., Lee, T.Y., Zhang, Y.Q., Xie, Y.W., Li, X.H., Wang, K.L., Wang, P.L., 1998. Diachronous uplift of the Tibetan plateau starting 40 Myr ago. Nature 394, 769–773.
Clark, M.K., Schoenbohm, L.M., Royden, L.H., Whipple, K.X., Burchfiel, B.C., Zhang, X., Tang, W., Wang, E., Chen, L., 2004. Surface uplift, tectonics, and erosion of eastern Tibet from large-scale drainage patterns. Tectonics 23, 1–20.
Fan, D., Li, C., Yokoyama, K., Zhou, B., Li, B., Wang, Q., Yang, S., Deng, B., Wu, G., 2005. Monazite age spectra in the late Cenozoic strata of the Changjiang delta and its implication on the Changjiang run-through time. Sci. China Ser. D Earth Sci. 48, 1718–1727.
Fu, X.W., Zhu, W.L., Geng, J.H., Yang, S.Y., Zhong, K., Huang, X.T., Zhang, L.Y., Xu, X., 2021. The present-day Yangtze River was established in the late Miocene: evidence from detrital zircon ages. J. Asian Earth Sci. 205, 104600.
Granger, D.E., 2006. A review of burial dating methods using 26Al and 10Be. Geol. Soc. Am. Spec. Pap. 415, 1–16.
Granger, D.E., 2014. Cosmogenic nuclide burial dating in archaeology and paleoanthropology. In: Turekian, K., Holland, H. (Eds.), Treatise on Geochemistry, , second edvol. 14. Elsevier Publishing, pp. 81–97.
Granger, D.E., Muzikar, P.F., 2001. Dating sediment burial with in situ-produced cosmogenic nuclides: theory, techniques, and limitations. Earth Planet. Sci. Lett. 188, 269–281.
Gu, J.W., Chen, J., Sun, Q.L., Wang, Z.H., Wei, Z.X., Chen, Z.Y., 2014. China's Yangtze River Delta: geochemical fingerprints reflecting river connection to the sea. Geomorphology 227, 166–173.
Heisinger, B., Lal, D., Jull, A., Kubik, P., Ivy-Ochs, S., Neumaier, S., Knie, K., Lazarev, V., Nolte, E., 2002a. Production of selected cosmogenic radionuclides by muons: 1. Fast muons. Earth Planet. Sci. Lett. 200, 345–355.
Heisinger, B., Lal, D., Jull, A., Kubik, P., Ivy-Ochs, S., Knie, K., Nolte, E., 2002b. Production of selected cosmogenic radionuclides by muons: 2. Capture of negative muons. Earth Planet. Sci. Lett. 200, 357–369.
Hilgen, F.J., Lourens, L.J., Van Dam, J.A., 2012. The Neogene period. In: Gradstein, F.M., Ogg, J.G., Schmitz, M.D., et al. (Eds.), The Geological Time Scale 2012. Elsevier, Boston, pp. 923–978.
Jin, X., Yu, P., 1982. In: Geology of the Yellow Sea and the East China Sea. Science Press, Beijing, pp. 1–22 (in Chinese).
Kohl, C.P., Nishiizumi, K., 1992. Chemical isolation of quartz for measurement of in-situ-produced cosmogenic nuclides. Geochim. Cosmochim. Acta 56, 3583–3587.
Li, B., Wei, Z., Li, X., He, Z., Zhang, K., Wang, Z., 2011. Records from quaternary sediment and palaeo-environment in the Yangtze River delta. Quat. Sci. 31, 316–325 (in Chinese).
Liu, X.B., 2018. The Study of Magnetic Properties of Late Cenozoic Sediments on South and North Flanks of Yangtze River Delta: Source-sink Implications for River's Connection to the Sea. PH.D Thesis. East China Normal University (in Chinese with English abstract).
Liu, Y., Wang, S.J., Xu, S., Fabel, D., Liu, X.M., Zhang, X.B., Luo, W.J., Cheng, A.Y., 2013. New evidence for the incision history of the Liuchong River, Southwest China, from cosmogenic 26Al/10Be burial ages in cave sediments. J. Asian Earth Sci. 73, 274–283.
Liu, J.X., Liu, Q.S., Zhang, X.H., Liu, J., Wu, Z.Q., Mei, X., Shi, X.F., Zhao, Q.H., 2016. Magnetostratigraphy of a long quaternary sediment core in the south Yellow Sea. Quat. Sci. Rev. 144, 1–15.
Liu, J., Shi, X., Liu, Q., Ge, S., Liu, Y., Yao, Z., Zhao, Q., Jin, C., Jiang, Z., Liu, S., Qiao, S., Li, X., Li, C., Wang, C., 2014. Magnetostratigraphy of a greigite-bearing core from the South Yellow Sea: implications for re-magnetization and sedimentation. J. Geophys. Res. 119, 7425–7441.
Liu, X.B., Chen, J., Maher, B.A., Zhao, B.C., Yue, W., Sun, Q.L., Chen, Z.Y., 2018. Connection of the proto-Yangtze River to the East China Sea traced by sediment magnetic properties. Geomorphology 303, 162–171.
Masarik, J., Reedy, R.C., 1995. Terrestrial cosmogenic nuclide production systematic calculated from numerical simulations. Earth Planet. Sci. Lett. 136, 381–395.
McPhillips, D., Hoke, G.D., Zeng-Liu, J., Bierman, P.R., Rood, D.H., Niedermann, S., 2016. Dating the incision of the Yangtze River gorge at the First Bend using three-nuclide burial ages. Geophys. Res. Lett. 43, 101–110.
Mei, X., Li, R., Zhang, X., Liu, Q., Liu, J., Wang, Z., Lan, X., Liu, J., Sun, R., 2016. Evolution of the Yellow Sea warm current and the Yellow Sea cold water mass since the middle Pleistocene. Palaeogeogr. Palaeoclimatol. Palaeoecol. 442, 48–60.
Molnar, P., Tapponnier, P., 1975. Cenozoic tectonics of Asia: effects of continental collision. Science 189, 419–426.
Molnar, P., England, P., Martinod, J., 1993. Mantle dynamics, the uplift of the Tibetan Plateau and the indian monsoon. Rev. Geophys. 31, 357–396.
Morton, A.C., 1984. Stability of detrital heavy tertiary sandstones from sea basin minerals in the North Sea Basin. Clay Miner. 19, 287–308.
Nishiizumi, K., 2004. Preparation of 26Al AMS standards. Nucl. Inst. Methods Phys. Res. B 223, 388–392.
Pillans, B., Gibbard, P., 2012. The Quaternary period. In: Gradstein, F.M., Ogg, J.G., Schmitz, M.D., et al. (Eds.), The Geologic Time Scale 2012. Elsevier, Boston, pp. 979–1010.
Qiang, J., Weifeng, W., Huaimin, X., Shaochun, Y., Ji, Q., 1997. North Jiangsu Basin, eastern China: accumulation of immature oils and diagenesis of Paleogene reservoir rocks. J. Pet. Geol. 20, 287–306.
Qin, Y., Zhao, Y., Chen, L., Zhao, S., 1989. In: Geology of the Yellow Sea. Oceanic Publish House, Beijing, pp. 1–289 (in Chinese).
Ren, J.Y., Tamaki, K., Li, S.T., Zhang, J.X., 2002. Late Mesozoic and Cenozoic rifting and its dynamic setting in Eastern China and adjacent areas. Tectonophysics 344, 175–205.
Richardson, N.J., Densmore, A.L., Seward, D., Fowler, A., Wipf, M., Ellis, M.A., Li, Y., Zhang, Y., 2008. Extraordinary denudation in the Sichuan Basin: insights from low-temperature thermochronology adjacent to the eastern margin of the Tibetan Plateau. J. Geophys. Res. 113, B04409.
Saito, Y., Yang, Z.S., Hori, K., 2001. The Huanghe (Yellow River) and Changjiang (Yangtze River) deltas: a review on their characteristics, evolution and sediment discharge during the Holocene. Geomorphology 41, 219–231.
Shao, L., Yuan, S.Y., Li, C.A., Kang, C.G., Zhu, W.J., Liu, Y.D., Wang, J.T., 2015. Changing provenance of late Cenozoic sediments in the Jianghan Basin. Geosci. Front. 6, 605–615.
Tapponnier, P., Xu, Z.Q., Roger, F., Meyer, B., Arnaud, N., Wittlinger, G., Yang, J.S., 2001. Oblique stepwise rise and growth of the Tibet Plateau. Science 294, 1671–1677.
Wageman, J.M., Hilde, T.W., Emery, K., 1970. Structural framework of East China Sea and Yellow Sea. Am. Assoc. Pet. Geol. Bull. 54, 1611–1643.
Wang, P.X., 2004. Cenozoic deformation and the history of sea land interactions in Asia. In: Clift, P. (Ed.), Continent-Ocean Interactions in the East Asian Marginal Seas, Geophys. Monogr. Ser, vol. 149. AGU, Washington, D. C, pp. 1–22.
Wang, Z., Yang, S., Li, P., Li, C., Cai, J., 2006. Detrital mineral compositions of the Changjiang River sediments and their tracing implications. Acta Sedimentol. Sin. 24, 570–578.
Wang, C.S., Zhao, X.X., Liu, Z.F., Lippert, P.C., Graham, S.A., Coe, R.S., Yi, H.S., Zhu, L. D., Liu, S., Li, Y.L., 2008. Constraints on the early uplift history of the Tibetan Plateau. PNAS 105, 4987–4992.
Wang, P., Zheng, H.B., Chen, L., Chen, J., Xu, Y., Wei, X., Yao, X., 2014. Exhumation of the Huangling anticline in the Three Gorges region: Cenozoic sedimentary record from the western Jianghan Basin, China. Basin Res. 26, 505–522.
Xu, S., Freeman, S., Rood, D.H., Shanks, R.P., 2015. Decadal 10Be, 26Al and 36Cl QA measurements on the SUERC 5 MV accelerator mass spectrometer. Nucl. Inst. Methods Phys. Res. B 361, 39–42.
Yang, S., Li, C., Yokoyama, K., 2006. Elemental compositions and monazite age patterns of core sediments in the Changjiang Delta: implications for sediment provenance and development history of the Changjiang River. Earth Planet. Sci. Lett. 245, 762–776.
Yi, L., Ye, X., Chen, J., Li, Y., Long, H., Wang, X., Du, J., Zhao, S., Deng, C., 2014. Magnetostratigraphy and luminescence dating on a sedimentary sequence from northern East China Sea: constraints on evolutionary history of eastern marginal seas of China since the early Pleistocene. Quat. Int. 349, 316–326.
Yi, L., Deng, C., Tian, L., Xu, X., Jiang, X., Qiang, X., Qin, H., Ge, J., Chen, G., Su, Q., 2016. Plio-Pleistocene evolution of Bohai basin (East Asia): demise of Bohai paleolake and transition to marine environment. Sci. Report. 6, 29403.
Yu, J.J., Yue, W., Liu, P., Peng, B., Zhang, J., Sun, D.D., Wang, J.L., Lv, H.L., Chen, J., 2020. Provenance shift during the Plio-Pleistocene in the Vertex of Yangtze River Delta and its geomorphological implications. Minerals. https://doi.org/10.3390/min10110996.
Yue, W., Liu, J.T., Zhang, D., Wang, Z.H., Zhao, B.C., Chen, Z.Y., Chen, J., 2016. Magnetite with anomalously high Cr2O3 as a fingerprint to trace upper Yangtze sediments to the sea. Geomorphology 268, 14–20.
Yue, W., Yang, S., Zhao, B., Chen, Z., Yu, J., Liu, X., Huang, X., Jin, B., Chen, J., 2019. Changes in environment and provenance within the Changjiang (Yangtze River) Delta during Pliocene to Pleistocene transition. Mar. Geol. 416, 105976.
Zhang, Y.F., Li, C.A., Wang, Q.L., Chen, L., Ma, Y.F., Kang, C.G., 2008. Magnetism parameters characteristics of drilling deposits in Jianghan Plain and indication for forming of the Yangtze River Three Gorges. Chin. Sci. Bull. 53, 584–590.
Zhang, J., Wan, S.M., Clift, P.D., Huang, J., Yu, Z.J., Zhang, K.D., Mei, X., Liu, J., Han, Z. Y., Nan, Q.Y., Zhao, D.B., Li, A.C., Chen, L.H., Zheng, H.B., Yang, S.Y., Li, T.G., Zhang, X.H., 2019. History of Yellow River and Yangtze River delivering sediment to the Yellow Sea since 3.5 Ma: tectonic or climate forcing? Quat. Sci. Rev. 216, 74–88.
Zheng, H.B., Clift, P.D., Wang, P., Tada, R., Jia, J.T., He, M.Y., Jourdan, F., 2013. Pre-Miocene birth of the Yangtze River. PNAS 110, 7556–7561.